

Received 13 March 2017

Accepted 20 March 2017

Edited by W. T. A. Harrison, University of  
Aberdeen, Scotland

‡ Additional correspondence author, e-mail:  
j.wardell@abdn.ac.uk.

**Keywords:** crystal structure; carboxylate; salt;  
hydrogen bonding; Hirshfeld surface analysis.

**CCDC reference:** 1538892

**Supporting information:** this article has  
supporting information at journals.iucr.org/e

# Hydrazinium 2-amino-4-nitrobenzoate dihydrate: crystal structure and Hirshfeld surface analysis

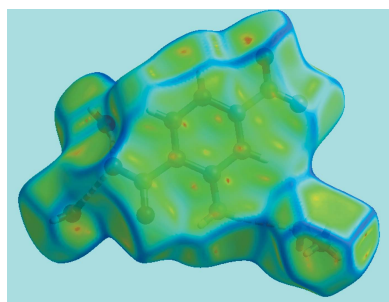
James L. Wardell,<sup>a,b,‡</sup> Mukesh M. Jotani<sup>c</sup> and Edward R. T. Tiekink<sup>d\*</sup>
<sup>a</sup>Fundação Oswaldo Cruz, Instituto de Tecnologia em Fármacos-Far Manguinhos 21041-250 Rio de Janeiro, RJ, Brazil,

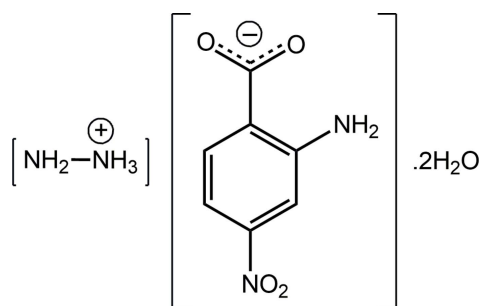
<sup>b</sup>Department of Chemistry, University of Aberdeen, Old Aberdeen, AB24 3UE, Scotland, <sup>c</sup>Department of Physics, Bhavan's Sheth R. A. College of Science, Ahmedabad, Gujarat 380 001, India, and <sup>d</sup>Research Centre for Chemical Crystallography, School of Science and Technology, Sunway University, 47500 Bandar Sunway, Selangor Darul Ehsan, Malaysia. \*Correspondence e-mail: edwardt@sunway.edu.my

In the anion of the title salt hydrate,  $\text{H}_5\text{N}_2^+ \cdot \text{C}_7\text{H}_5\text{N}_2\text{O}_4^- \cdot 2\text{H}_2\text{O}$ , the carboxylate and nitro groups lie out of the plane of the benzene ring to which they are bound [dihedral angles = 18.80 (10) and 8.04 (9)°, respectively], and as these groups are conrotatory, the dihedral angle between them is 26.73 (15)°. An intramolecular amino-N—H...O(carboxylate) hydrogen bond is noted. The main feature of the crystal packing is the formation of a supramolecular chain along the *b* axis, with a zigzag topology, sustained by charge-assisted water-O—H...O(carboxylate) hydrogen bonds and comprising alternating twelve-membered {...OCO...HOH}<sub>2</sub> and eight-membered {...O...HOH}<sub>2</sub> synthons. Each ammonium-N—H atom forms a charge-assisted hydrogen bond to a water molecule and, in addition, one of these forms a hydrogen bond with a nitro-O atom. The amine-N—H atoms form hydrogen bonds to carboxylate-O and water-O atoms, and the amine N atom accepts a hydrogen bond from an amino-H atom. The hydrogen bonds lead to a three-dimensional architecture. An analysis of the Hirshfeld surface highlights the major contribution of O...H/H...O hydrogen bonding to the overall surface, *i.e.* 46.8%, compared with H...H contacts (32.4%).

## 1. Chemical context

The present structure determination of the title salt dihydrate,  $[\text{NH}_2\text{NH}_3][\text{O}_2\text{C}_6\text{H}_4\text{NO}_2-4] \cdot 2\text{H}_2\text{O}$  (I), is a continuation of ongoing structural studies of the relatively unexplored chemistry of 2-amino-4-nitrobenzoic acid. This acid carries several groups capable of hydrogen bonding, *viz.* carboxylic/carboxylate, amino and even nitro, and is anticipated to form crystals with significant hydrogen-bonding interactions, in both its neutral and deprotonated forms. Beyond the structure determination of several polymorphs of the parent structure (Wardell & Tiekink, 2011; Wardell & Wardell, 2016) and its 1:1 co-crystal with bis(pyridin-2-yl)methanone and 2:1 co-crystal with 2-amino-4-nitrobenzoic acid (Wardell & Tiekink, 2011), all other investigations have been of deprotonated forms of the acid. Thus, the anion has been found coordinating in the carboxylate-O, amino-N mode towards  $\text{Pb}^{\text{II}}$  in the coordination polymer *catena*-[bis( $\mu_2$ -2-amino-4-nitrobenzoato)-lead(II)] (Chen & Huang, 2009), with the remaining literature structures being salts. These are either alkali metal salts, *i.e.*  $\text{Na}^+$ ,  $\text{K}^+$  (Smith, 2013),  $\text{Rb}^+$  (Smith, 2014*a*) and  $\text{Cs}^+$  (Smith & Wermuth, 2011), or are ammonium salts, as discussed below. Herein, the crystal and molecular structures of (I) are described along with an evaluation of its Hirshfeld surface.





## 2. Structural commentary

The molecular structures of the constituents of (I) are shown in Fig. 1; the asymmetric unit comprises one hydrazinium cation, one 2-amino-4-nitrobenzoate anion and two water molecules of crystallization. In all-organic structures, when protonated in crystals, hydrazine is ten times more likely to be present as a mono-protonated hydrazinium cation rather than in its the diprotonated form, *i.e.* hydrazine-1,2-diium di-cation (Groom *et al.*, 2016); when non-organic structures are also considered, this ratio increases to 20:1. The confirmation of the mono-protonation in (I) is found in the pattern of intermolecular interactions, in particular in the observation that the amine-N4 atom accepts a hydrogen bond (see below). The N3—N4 bond length in (I) is 1.4492 (15) Å. The assignment of deprotonation of 2-amino-4-nitrobenzoic acid during co-crystallization is readily adduced in the near equivalence of the carboxylate C—O bond lengths, *i.e.* C7—O1 = 1.2579 (15) and C7—O2 = 1.2746 (15) Å. While there is an intramolecular amino-N—H...O(carboxylate) hydrogen bond, Table 1, a significant twist of the carboxylate group with respect to the benzene ring to which it is connected is noted, as evidenced in the value of the C2—C1—C7—O1 torsion angle of 18.83 (17)°. With respect to the nitro group, this is also twisted

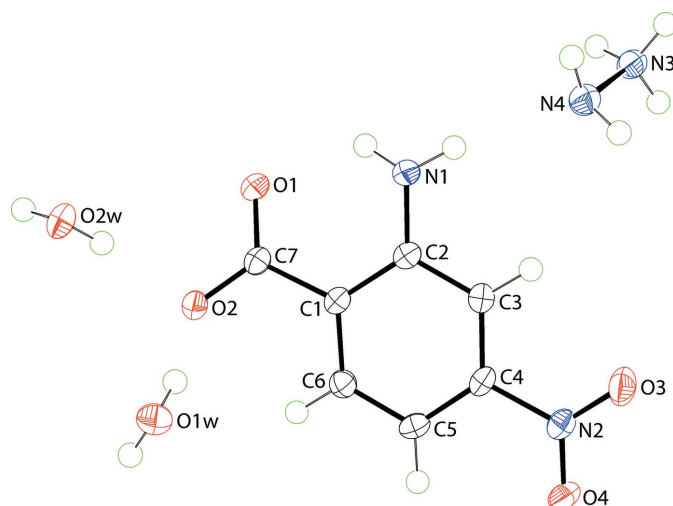


**Figure 1**  
The molecular structures of the asymmetric unit of (I), showing displacement ellipsoids at the 70% probability level.

**Table 1**  
Hydrogen-bond geometry (Å, °).

<i>D</i> —H... <i>A</i>	<i>D</i> —H	H... <i>A</i>	<i>D</i> ... <i>A</i>	<i>D</i> —H... <i>A</i>
N1—H1N...O1	0.88 (1)	2.07 (1)	2.7098 (15)	129 (1)
N1—H2N...N4	0.88 (1)	2.29 (1)	3.1403 (16)	165 (1)
N3—H3N...O1W <sup>i</sup>	0.86 (1)	1.97 (1)	2.8136 (15)	167 (1)
N3—H4N...O2W <sup>i</sup>	0.87 (2)	2.25 (2)	2.8969 (16)	132 (1)
N3—H4N...O4 <sup>ii</sup>	0.87 (2)	2.34 (1)	3.0739 (15)	143 (1)
N3—H5N...O2W <sup>iii</sup>	0.87 (1)	1.93 (2)	2.7862 (15)	167 (1)
N4—H6N...O1 <sup>iii</sup>	0.87 (1)	2.20 (1)	3.0623 (15)	178 (1)
N4—H7N...O1W <sup>iv</sup>	0.87 (1)	2.20 (1)	3.0106 (15)	155 (1)
O1W—H1W...O2	0.86 (2)	1.97 (2)	2.8071 (14)	166 (2)
O1W—H2W...O2 <sup>v</sup>	0.83 (2)	1.90 (2)	2.7208 (13)	171 (2)
O2W—H3W...O2	0.85 (2)	1.92 (2)	2.7479 (13)	165 (2)
O2W—H4W...O1 <sup>vi</sup>	0.85 (2)	1.91 (2)	2.7627 (14)	175 (2)

Symmetry codes: (i) *x*, *y*, *z* + 1; (ii) *x*, *y* + 1, *z*; (iii) *−x*, *−y* + 1, *−z* + 1; (iv) *−x*, *−y*, *−z* + 1; (v) *−x* + 1, *−y*, *−z*; (vi) *−x* + 1, *−y* + 1, *−z*.

but, to a lesser extent: the O3—N2—C4—C3 torsion angle is 7.53 (16)°. The terminal groups are conrotatory, forming a dihedral angle of 26.73 (15)°.

## 3. Supramolecular features

As expected from the chemical composition of (I), there are a number of conventional hydrogen-bonding interactions in the crystal, involving all possible hydrogen-bond donors and acceptors, Table 1. These sustain a three-dimensional architecture. A view of the interactions involving the hydrazinium cation is shown in Fig. 2*a*. Each of the ammonium-N3—H atoms forms a charge-assisted hydrogen bond to a water molecule, with the HN4 atom also forming a hydrogen bond to a nitro-O4 atom indicating that the HN4 atom is bifurcated [*i.e.*: N—H...O(O)]. The amine-N4—H atoms form a hydrogen bond to a carboxylate-O1 atom and to a water molecule and at the same time accept a hydrogen bond from an amino-H atom, this being the only N—H...N hydrogen bond in the structure; the second amino-H atom forms an intramolecular hydrogen bond with the carboxylate-O1 atom, as mentioned above. Each of the water-H atoms forms a charge-assisted hydrogen bond with a carboxylate-O atom, leading to a zigzag supramolecular chain aligned along the *b* axis, as shown in Fig. 2*b*. The chain comprises alternating twelve-membered {...OCO...HOH}<sub>2</sub> and eight-membered {...O...HOH}<sub>2</sub> synthons. As shown in Fig. 2*c*, two of the ammonium-N3—H atoms bridge water molecules in the chain shown in Fig. 2*b* to form a non-symmetric, eight-membered {...HNH...OH...O...HO} synthon while the amine-H atoms provide a second bridge between water- and carboxylate-O atoms to form a ten-membered {...HNH...OH...O...HOH...O} synthon. Further hydrogen bonds to water molecules leads to the formation of additional synthons, *i.e.* ten-membered {...HNNH...O}<sub>2</sub> and eight-membered {...HNH...O}<sub>2</sub>. A view of the unit-cell contents is shown in Fig. 2*d*. In addition to the above,  $\pi$ (phenyl)— $\pi$ (phenyl) interactions are noted between inversion-related rings with the inter-centroid separation being 3.6190 (8) Å [symmetry operation 1 − *x*, −*y*, 1 − *z*].

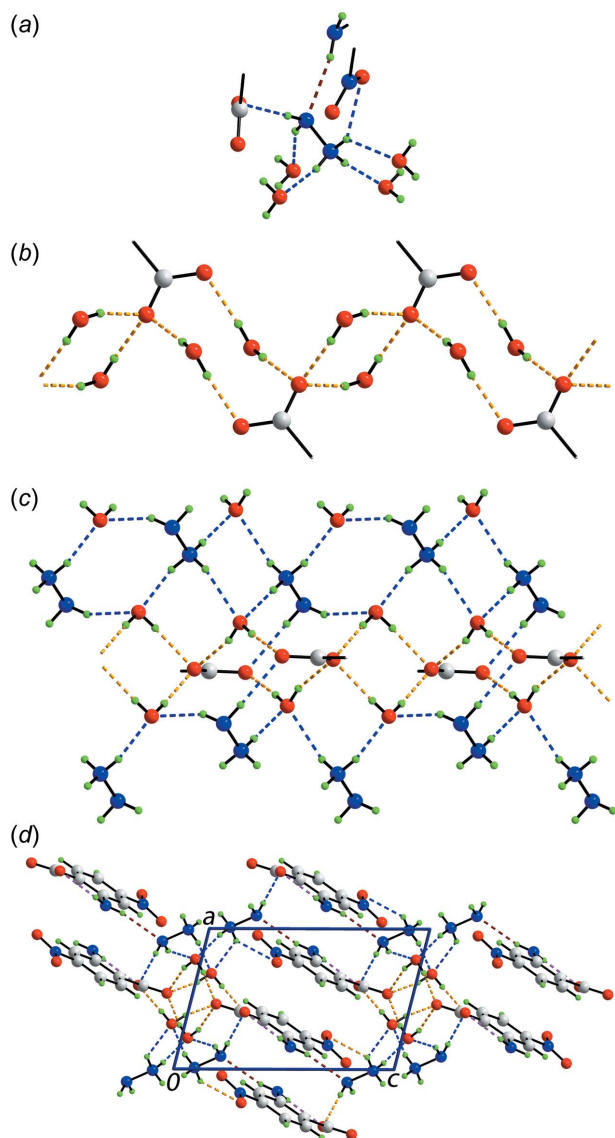


Figure 2

The molecular packing in (I): (a) immediate environment about the [H<sub>2</sub>NNH<sub>3</sub>]<sup>+</sup> cation, (b) supramolecular chain comprising anions and water molecules only, orientated along the *b* axis and sustained by water-O—H...O(carboxylate) hydrogen bonding, (c) decoration of the chain of (b) with cations and additional water molecules to highlight the formation of various supramolecular synthons (see text) and (d) a view of the unit-cell contents in projection down the *b* axis. The O—H...O, N—H...O, N—H...N and intramolecular N—H...O hydrogen bonds are shown as orange, blue, brown and pink dashed lines, respectively. In (b) and (c), all but the CO<sub>2</sub> groups of the two central benzoate residues have been removed for clarity.

#### 4. Hirshfeld surface analysis

The Hirshfeld surface analysis of (I) provides additional insight into its molecular packing and was performed in accord with a recent study of related ammonium salts (Wardell *et al.*, 2016). The Hirshfeld surface mapped over electrostatic potential in Fig. 3 highlights the positive potential (blue region) around the hydrazinium cation and the negative potential (red) about the carboxylate-oxygen atoms of the nitrobenzoate anion. The numerous bright-, diminutive- and

faint-red spots appearing on the Hirshfeld surface mapped over  $d_{\text{norm}}$  in Fig. 4 are indicative of the variety of intermolecular interactions in the crystal. The pair of charge-assisted water-O—H...O(carboxylate) hydrogen bonds between the water-O—H<sub>2</sub>W and —H<sub>4</sub>W atoms and carboxylate-O1 and -O2 atoms are evident through the bright-red spots appearing near the respective donor and acceptor atoms, Fig. 4a. The donors of these interactions appear as light-blue spots near the water O—H atoms and the acceptors as red regions surrounding carboxylate-O1 and -O2 atoms on the Hirshfeld surface mapped over electrostatic potential in Fig. 3.

The two pairs of bright-red spots near each water-O1W and -O2W atoms, and near the hydrazinium-H3N, H4N, H5N and H7N atoms in Fig. 4b are indicative of the hydrazinium-N—H...O(water) hydrogen bonds. In the same way, the amine-N4—H6N...O1 hydrogen bond is also viewed as a pair of bright-red spots near these atoms in Fig. 4b. The bifurcated ammonium-HN4 atom, forming comparatively weaker N—

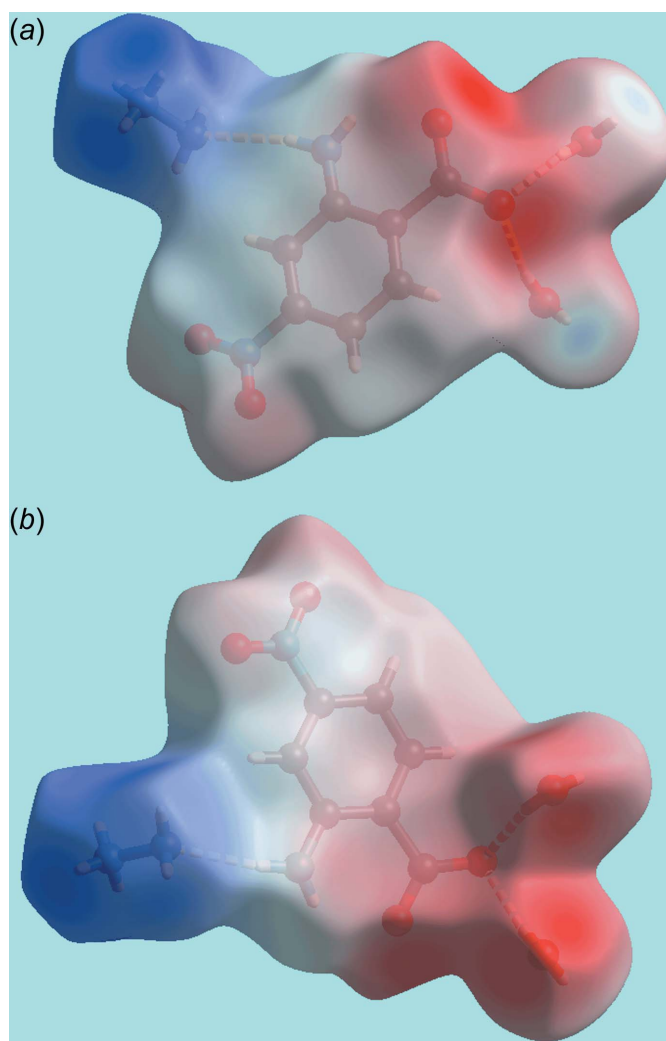


Figure 3

Two views of the Hirshfeld surface for (I) mapped over the electrostatic potential over the range  $-0.214$  to  $+0.341$  au; the red and blue regions represent negative and positive electrostatic potentials, respectively.

Table 2

Summary of short interatomic contacts (Å) in (I).

Contact	Distance	Symmetry operation
H5N...H3W	2.38 (2)	$-x, 1-y, 1-z$
H7N...H2W	2.34 (2)	$-x, -y, 1-z$
H4N...O3	2.626 (15)	$x, 1+y, z$
H5...O4	2.61	$1-x, -1-y, 1-z$
H2N...O4	2.652 (15)	$x, 1+y, z$
N1...O4	3.0205 (15)	$x, 1+y, z$
C7...O3	3.1231 (17)	$-x, -y, 1-z$
C2...C4	3.2936 (19)	$-x, -y, 1-z$
C3...C3	3.3235 (19)	$-x, -y, 1-z$

H...O hydrogen bonds compared to those just described, is viewed as the diminutive red spot in Fig. 4a. The presence of faint-red spots near the phenyl-C2–C4 atoms in Fig. 4b indicate their participation in edge-to-edge overlap with a symmetry-related phenyl ring, as seen in the short interatomic C...C contacts listed in Table 2. In addition to above intermolecular interactions, the crystal also features short interatomic C...O/O...C and N...O/O...N contacts, Table 2, which are viewed as very faint-red spots in Fig. 4. In Fig. 4b,

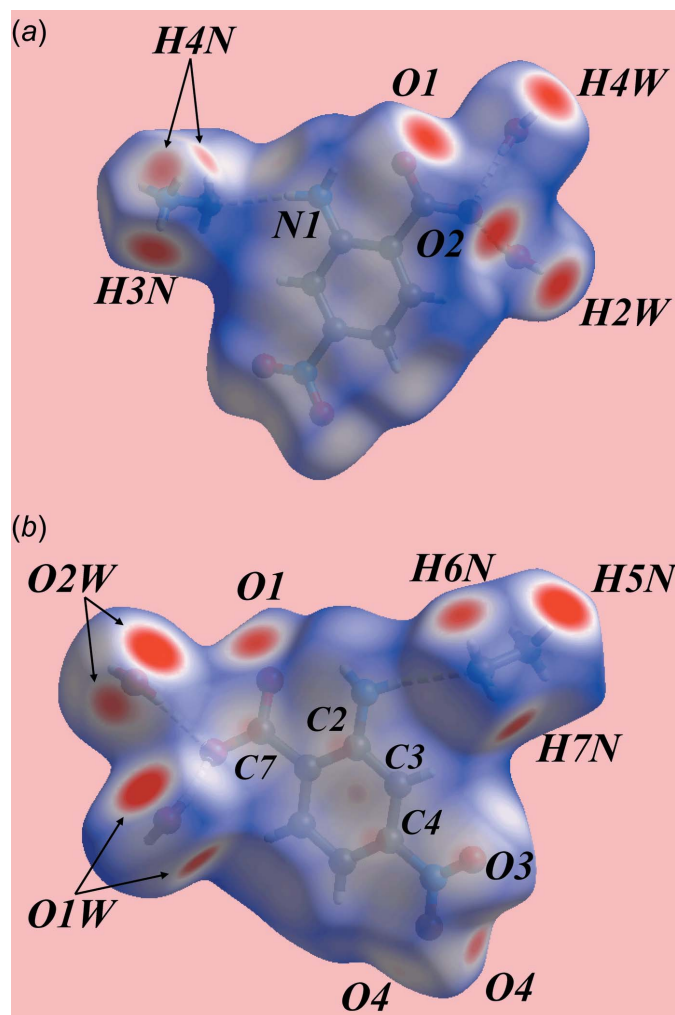


Figure 4

Two views of the Hirshfeld surface for (I) mapped over  $d_{\text{norm}}$  over the range  $-0.352$  to  $1.156$  au.

Table 3

Percentage contribution to interatomic contacts from the Hirshfeld surface for (I).

Contact	Percentage contribution
O...H/H...O	46.8
H...H	32.4
C...H/H...C	5.9
C...C	5.7
C...O/O...C	3.3
O...O	1.6
N...O/O...N	1.3
C...N / N...C	1.2
N...N	1.0
N...H/H...N	0.8

two spots are noted in the vicinity of the O4 atom, one corresponding to the conventional hydrogen bond and the other (to the left) to the weak H2N...O4 interaction, Table 2. The immediate environments about a reference ion-pair within the  $d_{\text{norm}}$ - and shape-index mapped Hirshfeld surfaces

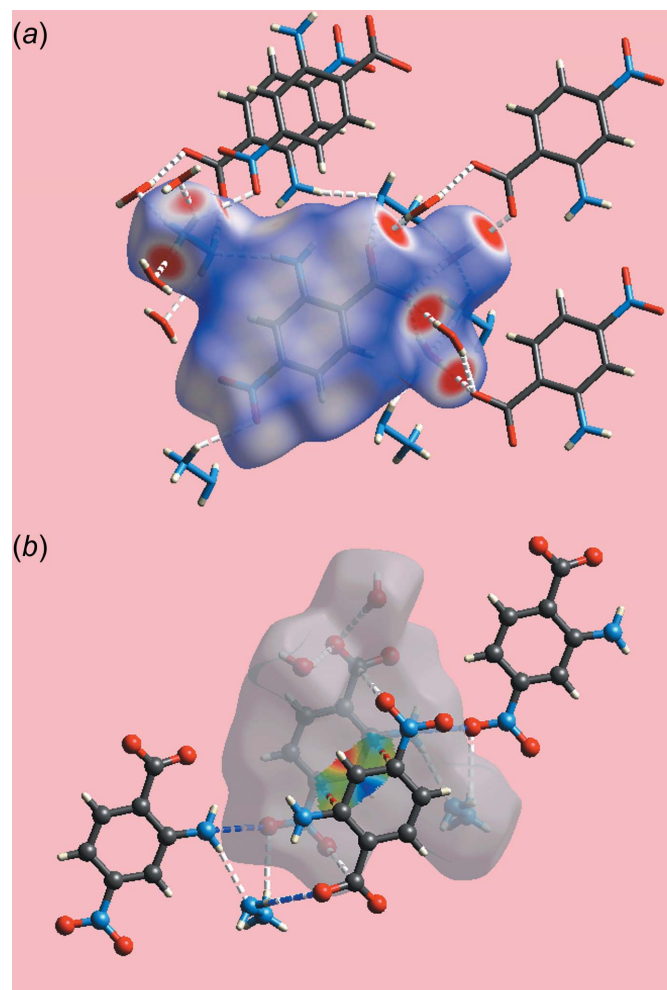


Figure 5

View of Hirshfeld surface for (I) mapped (a) over  $d_{\text{norm}}$  about a reference molecule showing hydrogen bonds as white dashed lines and (b) mapped with the shape-index property about a reference ion-pair. The short interatomic C...C, N...O and C...O contacts are indicated with red, blue and white dotted lines, respectively



highlighting the  $\text{O}-\text{H}\cdots\text{O}$  and  $\text{O}-\text{H}\cdots\text{N}$  hydrogen bonds, and short interatomic  $\text{C}\cdots\text{C}$ ,  $\text{C}\cdots\text{O}/\text{O}\cdots\text{C}$  and  $\text{N}\cdots\text{O}/\text{O}\cdots\text{N}$  contacts are illustrated in Fig. 5*a* and 5*b*, respectively.

The overall two-dimensional fingerprint plot for (I) and those delineated (McKinnon *et al.*, 2007) into  $\text{O}\cdots\text{H}/\text{H}\cdots\text{O}$ ,  $\text{H}\cdots\text{H}$ ,  $\text{C}\cdots\text{C}$ ,  $\text{C}\cdots\text{H}/\text{H}\cdots\text{C}$ ,  $\text{C}\cdots\text{O}/\text{O}\cdots\text{C}$  and  $\text{N}\cdots\text{O}/\text{O}\cdots\text{N}$  contacts are illustrated in Fig. 6*a–g*, respectively; their relative contributions to the Hirshfeld surfaces are summarized in Table 3. It is important to note that the most significant contribution to the Hirshfeld surface in (I) comes from  $\text{O}\cdots\text{H}/\text{H}\cdots\text{O}$  contacts, *i.e.* 46.8%, due to the involvement of all the acidic hydrogen atoms in hydrogen bonds, mainly to oxygen, many of which are charge-assisted. Reflecting this dominance, sharp spikes are evident in the fingerprint plot delineated into  $\text{O}\cdots\text{H}/\text{H}\cdots\text{O}$  contacts shown in Fig. 6*b*. The pair of green spikes have their tips at  $d_e + d_i \sim 1.9$  Å and extend linearly up

to  $d_e + d_i \sim 2.3$  Å. The points merged within the plot up to  $d_e + d_i \sim 2.7$  Å indicate the presence of short interatomic  $\text{O}\cdots\text{H}/\text{H}\cdots\text{O}$  contacts, Table 2. The extensive hydrogen bonding is the cause of the relatively small percentage contribution to the Hirshfeld surface from  $\text{H}\cdots\text{H}$  contacts, *i.e.* 32.4%, Fig. 6*c*, as relatively few hydrogen atoms are available to form interatomic contacts. The pair of tips at  $d_e + d_i \sim 2.3$  Å in the mirror-reflected saw-tooth distribution are due to short interatomic  $\text{H}\cdots\text{H}$  contacts involving water- and hydrazinium-hydrogen atoms, Table 2. The distributions of points in the fingerprint plot delineated into  $\text{C}\cdots\text{C}$  contacts, shown in Fig. 6*d*, represents two  $\pi$ - $\pi$  stacking interactions. In the first of these, the symmetry-related phenyl rings have a face-to-face overlap to give the arrow-like distribution in lower ( $d_e$ ,  $d_i$ ) region at around  $d_e = d_i = 1.6$  Å. This interaction is also seen as the flat region appearing about the phenyl ring on the Hirshfeld surface mapped over curvedness, shown in Fig. 7. The other  $\pi$ - $\pi$  stacking interaction involves edge-to-edge overlap through short interatomic  $\text{C}\cdots\text{C}$  contacts involving the C2–C4 atoms, Fig. 4*b* and Table 2, and is viewed as the arrow-like distribution of points around  $d_e = d_i = 1.8$  Å, *i.e.* adjacent to first arrow-like distribution. Even though  $\text{C}\cdots\text{H}/\text{H}\cdots\text{C}$  contacts have a significant contribution to the Hirshfeld surface, *i.e.* 5.9%, as seen from the fingerprint plot in Fig. 6*e*, the interatomic separations are much greater than sum of their van der Waals radii and hence do not appear to have influence on the molecular packing. The presence of short interatomic  $\text{C}\cdots\text{O}/\text{O}\cdots\text{C}$  and  $\text{N}\cdots\text{O}/\text{O}\cdots\text{N}$  contacts in the crystal, Table 2, is also evident from the small but significant contributions of 3.3 and 1.3%, respectively, to the Hirshfeld surfaces and appear as pairs of forceps-like tips, Fig. 6*f*, and conical tips, Fig. 6*g*, at  $d_e + d_i \sim 3.1$  Å in their respective fingerprint plots. The small contributions from the other interatomic  $\text{O}\cdots\text{O}$ ,  $\text{C}\cdots\text{N}/\text{N}\cdots\text{C}$ ,  $\text{N}\cdots\text{N}$  and  $\text{N}\cdots\text{H}/\text{H}\cdots\text{N}$  contacts listed in Table 2 have a negligible effect on the packing in the crystal.

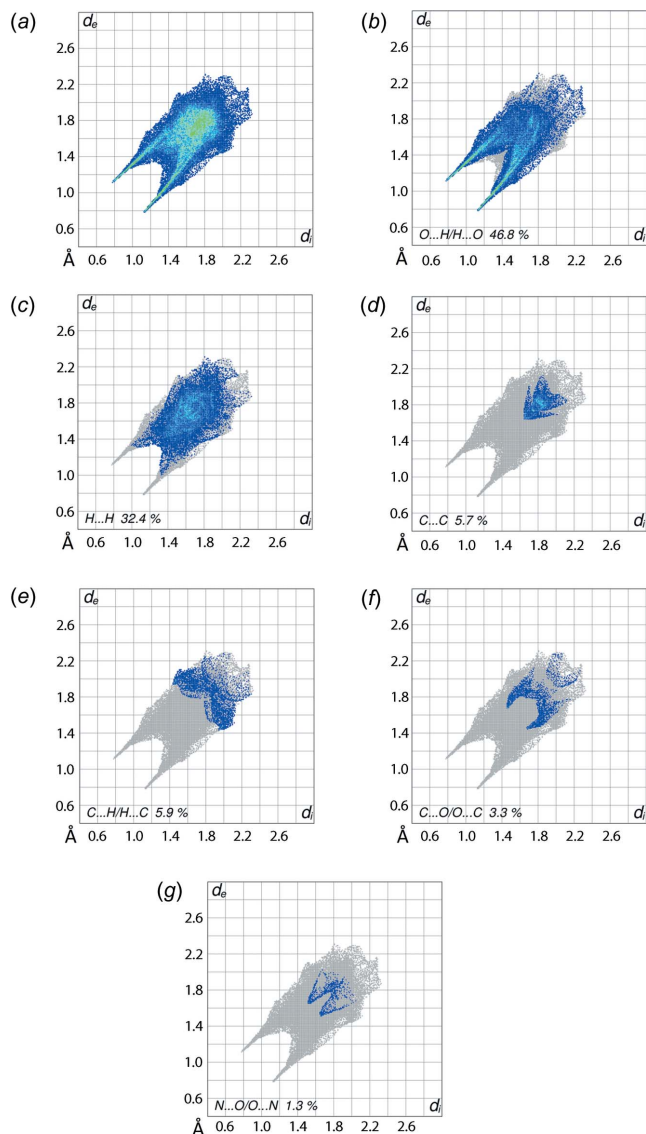


Figure 6

(*a*) The full two-dimensional fingerprint plot for (I) and fingerprint plots delineated into (*b*)  $\text{O}\cdots\text{H}/\text{H}\cdots\text{O}$ , (*c*)  $\text{H}\cdots\text{H}$ , (*d*)  $\text{C}\cdots\text{C}$ , (*e*)  $\text{C}\cdots\text{H}/\text{H}\cdots\text{C}$ , (*f*)  $\text{C}\cdots\text{O}/\text{O}\cdots\text{C}$  and (*g*)  $\text{N}\cdots\text{O}/\text{O}\cdots\text{N}$  contacts.

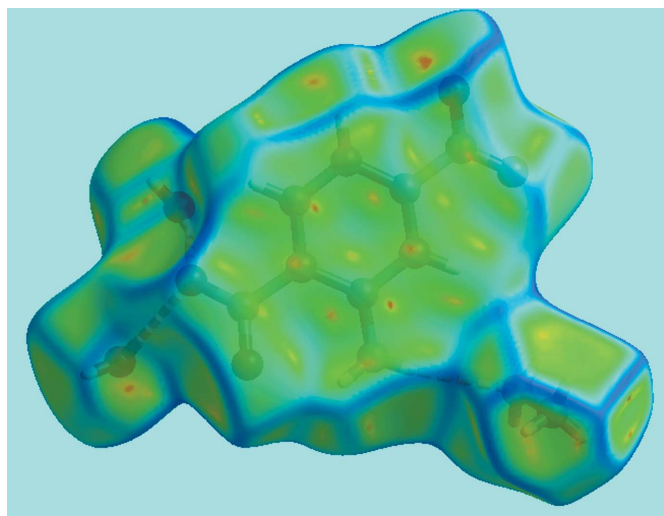


Figure 7

A view of Hirshfeld surfaces mapped over curvedness showing the flat region about the phenyl ring engaged in face-to-face  $\pi$ - $\pi$  interactions.

Table 4

Geometric data (°) for ammonium salts of 2-amino-4-nitrobenzoate. Extreme values for each parameter are bolded.

cation	Z'	C <sub>6</sub> /CO <sub>2</sub>	C <sub>6</sub> /NO <sub>2</sub>	CO <sub>2</sub> /NO <sub>2</sub>	Ref.
[NH <sub>4</sub> ] <sup>+</sup> <sup>a</sup>	1	<b>26.4 (3)</b>	2.9 (3)	24.1 (4)	Smith (2014b)
[Me <sub>2</sub> NH <sub>2</sub> ] <sup>+</sup>	1	11.45 (13)	3.71 (15)	7.9 (2)	Wardell <i>et al.</i> (2016)
[ <i>n</i> -Bu <sub>2</sub> NH <sub>2</sub> ] <sup>+</sup>	2	12.73 (6)	4.30 (10)	17.02 (8)	Wardell <i>et al.</i> (2016)
		8.1 (4)	<b>12.6 (3)</b>	19.0 (5)	
[Cy <sub>2</sub> NH <sub>2</sub> ] <sup>+</sup>	2	9.87 (10)	7.58 (15)	3.42 (19)	Smith <i>et al.</i> (2004)
		9.52 (9)	7.86 (11)	3.92 (2)	
[O(CH <sub>2</sub> CH <sub>2</sub> ) <sub>2</sub> NH <sub>2</sub> ] <sup>+</sup>	1	17.92 (9)	1.28 (11)	19.19 (13)	Smith & Lynch (2016)
[(H <sub>2</sub> N) <sub>2</sub> C=NH <sub>2</sub> ] <sup>+</sup> <sup>a</sup>	1	5.88 (11)	5.64 (12)		Smith <i>et al.</i> (2007)
[H <sub>3</sub> NCH <sub>2</sub> CH <sub>2</sub> NH <sub>3</sub> ] <sup>2+</sup> <sup>b</sup>	1	<b>3.44 (14)</b>	<b>0.69 (11)</b>	<b>3.2 (2)</b>	Smith <i>et al.</i> (2002)
[H <sub>2</sub> NNH <sub>3</sub> ] <sup>2+</sup> <sup>b</sup>	1	18.80 (10)	8.04 (9)	<b>26.73 (14)</b>	this work

Notes: (a) crystallized as a monohydrate; (b) crystallized as a dihydrate.

## 5. Database survey

In the *Chemical context* section above, it was indicated that in the crystallographic literature there are several ammonium salts of 2-amino-4-nitrobenzoate anions. The ammonium cations range from the simple ammonium cation (Smith, 2014b) to R<sub>2</sub>NH<sub>2</sub>, *i.e.* R = Me, *n*-Bu (Wardell *et al.*, 2016), Cy (Smith *et al.*, 2004) and R<sub>2</sub> = (CH<sub>2</sub>CH<sub>2</sub>)<sub>2</sub>O (Smith & Lynch, 2016). More exotic examples of ammonium cations are found with [(H<sub>2</sub>N)<sub>2</sub>C=NH<sub>2</sub>]<sup>+</sup>, *i.e.* guanidinium (Smith *et al.*, 2007) and the dication, [H<sub>3</sub>NCH<sub>2</sub>CH<sub>2</sub>NH<sub>3</sub>]<sup>2+</sup> (Smith *et al.*, 2002). Key geometric data for these are collated in Table 4. From these data it is apparent that the dihedral angle formed between the the carboxylate group and benzene ring in (I) is at the upper end of structures included in Table 4, and in the

same way, the angle between the nitro group and benzene ring is in the upper range of comparable angles. Given that the relationship between the carboxylate and nitro groups in (I) is conrotatory, the dihedral angle between these groups in (I), at 26.73 (14)°, is the greatest among the series.

## 6. Synthesis and crystallization

Solutions of 2-amino-4-nitrobenzoic acid (1 mmol) in MeOH (10 ml) and hydrazine (1 mmol) in MeOH (15 ml) were mixed and heated under reflux for 30 min. The reaction mixture was left at room temperatures for three days and the red blocks that formed were collected. M.p. 375–377 K (dec.). IR (KBr: cm<sup>-1</sup>): 3514(s), 3399(s), 3400–2500(*br,s*), 1680, 1553, 1526, 1425, 1359, 1276, 830, 733.

## 7. Refinement

Crystal data, data collection and structure refinement details are summarized in Table 5. Carbon-bound H-atoms were placed in calculated positions (C–H = 0.95–0.99 Å) and were included in the refinement in the riding-model approximation, with *U*<sub>iso</sub>(H) set to 1.2*U*<sub>eq</sub>(C). The O- and N-bound H atoms were located from difference maps, but refined with O–H = 0.84±0.01 Å and *U*<sub>iso</sub>(H) = 1.5*U*<sub>eq</sub>(O), and with N–H = 0.86–0.88±0.01 Å and *U*<sub>iso</sub>(H) = 1.2*U*<sub>eq</sub>(N), respectively. Owing to poor agreement, two reflections, *i.e.* (202) and (212), were omitted from the final cycles of refinement.

## Acknowledgements

The authors thank the National Crystallographic Service, based at the University of Southampton, for collecting the data. JLW thanks CNPq, Brazil, for a grant. The authors are also grateful to Sunway University (INT-RRO-2017-096) for supporting this research.

## References

- Brandenburg, K. (2006). *DIAMOND*. Crystal Impact GbR, Bonn, Germany.
- Chen, H.-L. & Huang, C.-F. (2009). *Synth. React. Inorg., Met.-Org., Nano-Met. Chem.* **39**, 533–536.
- Farrugia, L. J. (2012). *J. Appl. Cryst.* **45**, 849–854.

Table 5

Experimental details.

Crystal data	
Chemical formula	H <sub>5</sub> N <sub>2</sub> <sup>+</sup> ·C <sub>7</sub> H <sub>5</sub> N <sub>2</sub> O <sub>4</sub> <sup>−</sup> ·2H <sub>2</sub> O
<i>M</i> <sub>r</sub>	250.22
Crystal system, space group	Triclinic, <i>P</i> $\bar{1}$
Temperature (K)	120
<i>a</i> , <i>b</i> , <i>c</i> (Å)	6.9695 (2), 8.0960 (3), 10.5316 (3)
$\alpha$ , $\beta$ , $\gamma$ (°)	76.468 (2), 73.251 (2), 75.390 (2)
<i>V</i> (Å <sup>3</sup> )	542.23 (3)
<i>Z</i>	2
Radiation type	Mo <i>K</i> α
$\mu$ (mm <sup>-1</sup> )	0.13
Crystal size (mm)	0.41 × 0.22 × 0.13
Data collection	
Diffractionmeter	Bruker–Nonius Roper CCD camera on $\kappa$ -goniostat
Absorption correction	Multi-scan ( <i>SADABS</i> ; Sheldrick, 2007)
<i>T</i> <sub>min</sub> , <i>T</i> <sub>max</sub>	0.644, 0.746
No. of measured, independent and observed [ <i>I</i> > 2σ( <i>I</i> )] reflections	11539, 2497, 2147
<i>R</i> <sub>int</sub>	0.034
Refinement	
<i>R</i> [ <i>F</i> <sup>2</sup> > 2σ( <i>F</i> <sup>2</sup> )], <i>wR</i> ( <i>F</i> <sup>2</sup> ), <i>S</i>	0.039, 0.110, 1.05
No. of reflections	2497
No. of parameters	187
No. of restraints	13
Δρ <sub>max</sub> , Δρ <sub>min</sub> (e Å <sup>-3</sup> )	0.29, −0.30

Computer programs: *DENZO* (Otwinowski & Minor, 1997), *COLLECT* (Hooft, 1998), *SHELXS97* (Sheldrick, 2008), *SHELXL2014* (Sheldrick, 2015), *ORTEP-3 for Windows* (Farrugia, 2012) and *DIAMOND* (Brandenburg, 2006) and *publCIF* (Westrip, 2010).

- Groom, C. R., Bruno, I. J., Lightfoot, M. P. & Ward, S. C. (2016). *Acta Cryst.* **B72**, 171–179.
- Hooft, R. W. W. (1998). *COLLECT*. Nonius BV, Delft, The Netherlands.
- McKinnon, J. J., Jayatilaka, D. & Spackman, M. A. (2007). *Chem. Commun.* pp. 3814–3816.
- Otwinowski, Z. & Minor, W. (1997). *Methods in Enzymology*, Vol. 276, *Macromolecular Crystallography*, Part A, edited by C. W. Carter Jr & R. M. Sweet, pp. 307–326. New York: Academic Press.
- Sheldrick, G. M. (2007). *SADABS*. University of Göttingen, Germany.
- Sheldrick, G. M. (2008). *Acta Cryst.* **A64**, 112–122.
- Sheldrick, G. M. (2015). *Acta Cryst.* **C71**, 3–8.
- Smith, G. (2013). *Acta Cryst.* **C69**, 1472–1477.
- Smith, G. (2014a). *Acta Cryst.* **E70**, m192–m193.
- Smith, G. (2014b). Private communication (refcode DOBP1V). CCDC, Cambridge, England.
- Smith, G. & Lynch, D. E. (2016). *Acta Cryst.* **C72**, 105–111.
- Smith, G. & Wermuth, U. D. (2011). *Acta Cryst.* **E67**, m1047–m1048.
- Smith, G., Wermuth, U. D. & Healy, P. C. (2004). *Acta Cryst.* **E60**, o684–o686.
- Smith, G., Wermuth, U. D., Healy, P. C. & White, J. M. (2007). *Acta Cryst.* **E63**, o7–o9.
- Smith, G., Wermuth, U. D. & White, J. M. (2002). *Acta Cryst.* **E58**, o1088–o1090.
- Wardell, J. L., Jotani, M. M. & Tiekink, E. R. T. (2016). *Acta Cryst.* **E72**, 1618–1627.
- Wardell, J. L. & Tiekink, E. R. T. (2011). *J. Chem. Crystallogr.* **41**, 1418–1424.
- Wardell, S. M. S. V. & Wardell, J. L. (2016). *J. Chem. Crystallogr.* **46**, 34–43.
- Westrip, S. P. (2010). *J. Appl. Cryst.* **43**, 920–925.

## supporting information

*Acta Cryst.* (2017). E73, 579-585 [https://doi.org/10.1107/S2056989017004352]

## Hydrazinium 2-amino-4-nitrobenzoate dihydrate: crystal structure and Hirshfeld surface analysis

James L. Wardell, Mukesh M. Jotani and Edward R. T. Tiekink

### Computing details

Data collection: *COLLECT* (Hooft, 1998); cell refinement: *DENZO* (Otwinowski & Minor, 1997) and *COLLECT* (Hooft, 1998); data reduction: *DENZO* (Otwinowski & Minor, 1997) and *COLLECT* (Hooft, 1998); program(s) used to solve structure: *SHELXS97* (Sheldrick, 2008); program(s) used to refine structure: *SHELXL2014* (Sheldrick, 2015); molecular graphics: *ORTEP-3 for Windows* (Farrugia, 2012) and *DIAMOND* (Brandenburg, 2006); software used to prepare material for publication: *publCIF* (Westrip, 2010).

### Hydrazinium 2-amino-4-nitrobenzoate dihydrate

#### Crystal data

$\text{H}_5\text{N}_2^+ \cdot \text{C}_7\text{H}_5\text{N}_2\text{O}_4^- \cdot 2\text{H}_2\text{O}$

$M_r = 250.22$

Triclinic,  $P\bar{1}$

$a = 6.9695$  (2) Å

$b = 8.0960$  (3) Å

$c = 10.5316$  (3) Å

$\alpha = 76.468$  (2)°

$\beta = 73.251$  (2)°

$\gamma = 75.390$  (2)°

$V = 542.23$  (3) Å<sup>3</sup>

$Z = 2$

$F(000) = 264$

$D_x = 1.533$  Mg m<sup>-3</sup>

Mo  $K\alpha$  radiation,  $\lambda = 0.71073$  Å

Cell parameters from 7476 reflections

$\theta = 2.9\text{--}27.5^\circ$

$\mu = 0.13$  mm<sup>-1</sup>

$T = 120$  K

Block, red

$0.41 \times 0.22 \times 0.13$  mm

#### Data collection

Bruker–Nonius Roper CCD camera on  $\kappa$ -goniostat

diffractometer

Radiation source: Bruker–Nonius FR591

rotating anode

Graphite monochromator

Detector resolution: 9.091 pixels mm<sup>-1</sup>

$\varphi$  &  $\omega$  scans

Absorption correction: multi-scan (SADABS; Sheldrick, 2007)

$T_{\min} = 0.644$ ,  $T_{\max} = 0.746$

11539 measured reflections

2497 independent reflections

2147 reflections with  $I > 2\sigma(I)$

$R_{\text{int}} = 0.034$

$\theta_{\max} = 27.6^\circ$ ,  $\theta_{\min} = 3.1^\circ$

$h = -9 \rightarrow 8$

$k = -10 \rightarrow 10$

$l = -13 \rightarrow 13$

#### Refinement

Refinement on  $F^2$

Least-squares matrix: full

$R[F^2 > 2\sigma(F^2)] = 0.039$

$wR(F^2) = 0.110$

$S = 1.05$

2497 reflections

187 parameters

13 restraints

Hydrogen site location: mixed



$$w = 1/[\sigma^2(F_o^2) + (0.0646P)^2 + 0.1366P]$$

$$\text{where } P = (F_o^2 + 2F_c^2)/3$$

$$(\Delta/\sigma)_{\max} < 0.001$$

$$\Delta\rho_{\max} = 0.29 \text{ e } \text{\AA}^{-3}$$

$$\Delta\rho_{\min} = -0.30 \text{ e } \text{\AA}^{-3}$$

### Special details

**Geometry.** All esds (except the esd in the dihedral angle between two l.s. planes) are estimated using the full covariance matrix. The cell esds are taken into account individually in the estimation of esds in distances, angles and torsion angles; correlations between esds in cell parameters are only used when they are defined by crystal symmetry. An approximate (isotropic) treatment of cell esds is used for estimating esds involving l.s. planes.

### Fractional atomic coordinates and isotropic or equivalent isotropic displacement parameters ( $\text{\AA}^2$ )

	<i>x</i>	<i>y</i>	<i>z</i>	$U_{\text{iso}}^*/U_{\text{eq}}$
O1	0.40595 (14)	0.36669 (11)	0.25616 (9)	0.0168 (2)
O2	0.46220 (13)	0.18017 (11)	0.11781 (9)	0.0164 (2)
O3	0.04781 (14)	−0.28112 (12)	0.77375 (9)	0.0224 (2)
O4	0.24000 (15)	−0.47250 (11)	0.65475 (9)	0.0195 (2)
N1	0.15996 (17)	0.28747 (14)	0.50370 (11)	0.0163 (2)
H1N	0.218 (2)	0.3697 (17)	0.4483 (14)	0.020*
H2N	0.107 (2)	0.301 (2)	0.5877 (10)	0.020*
N2	0.17056 (16)	−0.32135 (13)	0.67034 (10)	0.0150 (2)
C1	0.34738 (18)	0.08075 (15)	0.35268 (12)	0.0128 (3)
C2	0.23062 (17)	0.12171 (15)	0.47960 (12)	0.0123 (3)
C3	0.17447 (18)	−0.01538 (16)	0.58371 (12)	0.0133 (3)
H3	0.0949	0.0079	0.6698	0.016*
C4	0.23572 (18)	−0.18300 (15)	0.55975 (12)	0.0132 (3)
C5	0.35262 (19)	−0.22781 (16)	0.43707 (13)	0.0152 (3)
H5	0.3943	−0.3450	0.4241	0.018*
C6	0.40531 (19)	−0.09256 (16)	0.33461 (12)	0.0148 (3)
H6	0.4836	−0.1183	0.2489	0.018*
C7	0.40929 (18)	0.21917 (15)	0.23517 (12)	0.0130 (3)
N3	−0.00982 (17)	0.32666 (14)	0.90634 (11)	0.0161 (2)
H3N	0.045 (2)	0.2268 (14)	0.9450 (14)	0.019*
H4N	0.086 (2)	0.3844 (19)	0.8652 (14)	0.019*
H5N	−0.102 (2)	0.3825 (19)	0.9655 (13)	0.019*
N4	−0.09239 (17)	0.30241 (15)	0.80197 (11)	0.0180 (3)
H6N	−0.179 (2)	0.3973 (15)	0.7857 (16)	0.022*
H7N	−0.159 (2)	0.2192 (17)	0.8375 (15)	0.022*
O1W	0.21973 (14)	0.02486 (12)	0.02803 (10)	0.0184 (2)
H1W	0.279 (3)	0.070 (2)	0.0681 (16)	0.028*
H2W	0.312 (2)	−0.033 (2)	−0.0235 (15)	0.028*
O2W	0.31998 (14)	0.45790 (12)	−0.06089 (9)	0.0170 (2)
H3W	0.381 (2)	0.382 (2)	−0.0080 (15)	0.025*
H4W	0.409 (2)	0.506 (2)	−0.1221 (15)	0.025*

### Atomic displacement parameters ( $\text{\AA}^2$ )

	$U^{11}$	$U^{22}$	$U^{33}$	$U^{12}$	$U^{13}$	$U^{23}$
O1	0.0211 (5)	0.0127 (5)	0.0162 (4)	−0.0063 (3)	−0.0025 (3)	−0.0008 (3)

O2	0.0197 (5)	0.0145 (5)	0.0126 (4)	−0.0027 (3)	−0.0020 (3)	−0.0008 (3)
O3	0.0216 (5)	0.0207 (5)	0.0165 (5)	−0.0019 (4)	0.0023 (4)	0.0019 (4)
O4	0.0268 (5)	0.0115 (5)	0.0204 (5)	−0.0057 (4)	−0.0067 (4)	0.0005 (3)
N1	0.0209 (6)	0.0119 (5)	0.0145 (5)	−0.0046 (4)	−0.0005 (4)	−0.0026 (4)
N2	0.0151 (5)	0.0145 (5)	0.0158 (5)	−0.0045 (4)	−0.0059 (4)	0.0009 (4)
C1	0.0127 (6)	0.0121 (6)	0.0139 (6)	−0.0033 (4)	−0.0043 (4)	−0.0004 (4)
C2	0.0113 (6)	0.0120 (6)	0.0147 (6)	−0.0027 (4)	−0.0058 (4)	−0.0009 (4)
C3	0.0122 (6)	0.0148 (6)	0.0126 (6)	−0.0031 (4)	−0.0033 (4)	−0.0012 (4)
C4	0.0129 (6)	0.0127 (6)	0.0140 (6)	−0.0046 (4)	−0.0052 (4)	0.0021 (5)
C5	0.0162 (6)	0.0102 (6)	0.0187 (6)	−0.0014 (4)	−0.0055 (5)	−0.0014 (5)
C6	0.0146 (6)	0.0148 (6)	0.0140 (6)	−0.0025 (4)	−0.0024 (4)	−0.0027 (5)
C7	0.0109 (6)	0.0129 (6)	0.0142 (6)	−0.0016 (4)	−0.0035 (4)	−0.0005 (4)
N3	0.0162 (5)	0.0139 (5)	0.0173 (6)	−0.0033 (4)	−0.0034 (4)	−0.0017 (4)
N4	0.0207 (6)	0.0166 (6)	0.0173 (6)	−0.0050 (4)	−0.0047 (4)	−0.0025 (4)
O1W	0.0177 (5)	0.0171 (5)	0.0203 (5)	−0.0020 (4)	−0.0038 (4)	−0.0056 (4)
O2W	0.0154 (4)	0.0169 (5)	0.0161 (5)	−0.0045 (3)	−0.0037 (3)	0.0029 (4)

*Geometric parameters (Å, °)*

O1—C7	1.2579 (15)	C4—C5	1.3886 (18)
O2—C7	1.2746 (15)	C5—C6	1.3855 (18)
O3—N2	1.2299 (14)	C5—H5	0.9500
O4—N2	1.2280 (14)	C6—H6	0.9500
N1—C2	1.3644 (16)	N3—N4	1.4492 (15)
N1—H1N	0.873 (9)	N3—H3N	0.864 (9)
N1—H2N	0.877 (9)	N3—H4N	0.865 (9)
N2—C4	1.4692 (15)	N3—H5N	0.872 (9)
C1—C6	1.4010 (17)	N4—H6N	0.864 (9)
C1—C2	1.4153 (17)	N4—H7N	0.865 (9)
C1—C7	1.5035 (16)	O1W—H1W	0.856 (14)
C2—C3	1.4106 (17)	O1W—H2W	0.834 (13)
C3—C4	1.3760 (18)	O2W—H3W	0.847 (13)
C3—H3	0.9500	O2W—H4W	0.852 (13)
C2—N1—H1N	118.5 (11)	C6—C5—H5	121.8
C2—N1—H2N	117.4 (10)	C4—C5—H5	121.8
H1N—N1—H2N	117.3 (15)	C5—C6—C1	122.44 (12)
O4—N2—O3	122.87 (10)	C5—C6—H6	118.8
O4—N2—C4	118.34 (10)	C1—C6—H6	118.8
O3—N2—C4	118.79 (10)	O1—C7—O2	123.11 (11)
C6—C1—C2	119.62 (11)	O1—C7—C1	119.32 (11)
C6—C1—C7	118.73 (11)	O2—C7—C1	117.57 (11)
C2—C1—C7	121.65 (11)	N4—N3—H3N	109.2 (10)
N1—C2—C3	118.52 (11)	N4—N3—H4N	105.8 (10)
N1—C2—C1	123.24 (11)	H3N—N3—H4N	108.1 (15)
C3—C2—C1	118.13 (11)	N4—N3—H5N	112.3 (10)
C4—C3—C2	119.56 (11)	H3N—N3—H5N	110.6 (15)
C4—C3—H3	120.2	H4N—N3—H5N	110.6 (15)

C2—C3—H3	120.2	N3—N4—H6N	105.4 (11)
C3—C4—C5	123.75 (11)	N3—N4—H7N	106.2 (11)
C3—C4—N2	117.70 (11)	H6N—N4—H7N	108.5 (16)
C5—C4—N2	118.54 (11)	H1W—O1W—H2W	106.4 (15)
C6—C5—C4	116.48 (11)	H3W—O2W—H4W	108.3 (15)
C6—C1—C2—N1	−176.80 (11)	O3—N2—C4—C5	−171.63 (11)
C7—C1—C2—N1	2.39 (18)	C3—C4—C5—C6	−0.98 (18)
C6—C1—C2—C3	−0.76 (17)	N2—C4—C5—C6	178.13 (10)
C7—C1—C2—C3	178.43 (10)	C4—C5—C6—C1	0.86 (18)
N1—C2—C3—C4	176.90 (11)	C2—C1—C6—C5	−0.02 (18)
C1—C2—C3—C4	0.67 (17)	C7—C1—C6—C5	−179.23 (11)
C2—C3—C4—C5	0.22 (18)	C6—C1—C7—O1	−161.98 (11)
C2—C3—C4—N2	−178.90 (10)	C2—C1—C7—O1	18.83 (17)
O4—N2—C4—C3	−173.12 (10)	C6—C1—C7—O2	18.36 (16)
O3—N2—C4—C3	7.53 (16)	C2—C1—C7—O2	−160.84 (11)
O4—N2—C4—C5	7.72 (16)		

Hydrogen-bond geometry (Å, °)

<i>D</i> —H... <i>A</i>	<i>D</i> —H	H... <i>A</i>	<i>D</i> ... <i>A</i>	<i>D</i> —H... <i>A</i>
N1—H1N...O1	0.88 (1)	2.07 (1)	2.7098 (15)	129 (1)
N1—H2N...N4	0.88 (1)	2.29 (1)	3.1403 (16)	165 (1)
N3—H3N...O1W <sup>i</sup>	0.86 (1)	1.97 (1)	2.8136 (15)	167 (1)
N3—H4N...O2W <sup>i</sup>	0.87 (2)	2.25 (2)	2.8969 (16)	132 (1)
N3—H4N...O4 <sup>ii</sup>	0.87 (2)	2.34 (1)	3.0739 (15)	143 (1)
N3—H5N...O2W <sup>iii</sup>	0.87 (1)	1.93 (2)	2.7862 (15)	167 (1)
N4—H6N...O1 <sup>iii</sup>	0.87 (1)	2.20 (1)	3.0623 (15)	178 (1)
N4—H7N...O1W <sup>iv</sup>	0.87 (1)	2.20 (1)	3.0106 (15)	155 (1)
O1W—H1W...O2	0.86 (2)	1.97 (2)	2.8071 (14)	166 (2)
O1W—H2W...O2 <sup>v</sup>	0.83 (2)	1.90 (2)	2.7208 (13)	171 (2)
O2W—H3W...O2	0.85 (2)	1.92 (2)	2.7479 (13)	165 (2)
O2W—H4W...O1 <sup>vi</sup>	0.85 (2)	1.91 (2)	2.7627 (14)	175 (2)

Symmetry codes: (i) *x*, *y*, *z*+1; (ii) *x*, *y*+1, *z*; (iii) −*x*, −*y*+1, −*z*+1; (iv) −*x*, −*y*, −*z*+1; (v) −*x*+1, −*y*, −*z*; (vi) −*x*+1, −*y*+1, −*z*.